

Prediction of Stroke Outcome in Mice Based on Non-Invasive MRI and Behavioral Testing

Felix Knab^{#1,2}, Stefan Paul Koch^{#1-3}, Sebastian Major^{1,2}, Tracy D. Farr¹⁻⁴, Susanne Mueller¹⁻³, Philipp Euskirchen¹, Moritz Eggers^{1,2}, Melanie T.C. Kuffner^{1,2}, Josefine Walter^{1,2,5}, Jens P. Dreier^{1,2,6-7}, Matthias Endres^{1,2,6,8-10}, Ulrich Dirnagl^{1,2,6,8-10}, Nikolaus Wenger^{1,2,6,11}, Christian J. Hoffmann^{1,2,11}, Philipp Boehm-Sturm^{#1-3}, Christoph Harms^{1,2,6,8,9,#}

¹Charité Universitätsmedizin Berlin, corporate member of Freie Universität Berlin and Humboldt-Universität zu Berlin, Klinik und Hochschulambulanz für Neurologie, Department of Experimental Neurology, Berlin, Germany

²Charité Universitätsmedizin Berlin, corporate member of Freie Universität Berlin and Humboldt-Universität zu Berlin, Center for Stroke Research Berlin, Charité Universitätsmedizin Berlin, Germany

³Charité Universitätsmedizin Berlin, corporate member of Freie Universität Berlin and Humboldt-Universität zu Berlin, NeuroCure Cluster of Excellence and Charité Core Facility 7T Experimental MRIs, Berlin, Germany

⁴School of Life Sciences, University of Nottingham, UK, NG7 2UH

⁵Berlin Institute of Health at Charité – Universitätsmedizin Berlin, QUEST Center for Transforming Biomedical Research, Berlin, Germany

⁶Einstein Center for Neuroscience, Berlin, Germany

⁷Bernstein Center for Computational Neuroscience

⁸German Center for Cardiovascular Research (DZHK), partner site Berlin

⁹NeuroCure Clinical Research Center, Charité-Universitätsmedizin Berlin, Berlin, Germany

¹⁰German Center for Neurodegenerative Diseases (DZNE)

¹¹Berlin Institute of Health (BIH), Berlin, Germany

#denotes equal contribution

Prediction of stroke outcome in mice

Correspondence to: Christoph Harms, Charité - Universitätsmedizin Berlin, Center for Stroke Research Berlin, Department of Experimental Neurology, Charitéplatz 1, 10117 Berlin, Germany

Fax number: +4930450 560942

Telephone Number: +4930450560631

Email address: christoph.harms@charite.de

Total word count: 6592

35 **ABSTRACT**

36 **Background:** Prediction of post-stroke outcome using the degree of subacute deficit or
37 magnetic resonance imaging is well studied in humans. While mice are the most commonly
38 used animals in preclinical stroke research, systematic analysis of outcome predictors is
39 lacking.

40 **Methods:** Data from 13 studies that included 45 min of middle cerebral artery occlusion on
41 148 mice were pooled. Motor function was measured using a modified protocol for the
42 staircase test of skilled reaching. Phases of subacute and residual deficit were defined.
43 Magnetic resonance images of stroke lesions were co-registered on the Allen Mouse Brain
44 Atlas to characterize stroke topology. Different random forest prediction models that either
45 used motor-functional deficit or imaging parameters were generated for the subacute and
46 residual deficits.

47 **Results:** We detected both a subacute and residual motor-functional deficit after stroke in
48 mice. Different functional severity grades and recovery trajectories could be observed. In
49 mice with small cortical lesions, lesion volume was the best predictor of the subacute deficit.
50 The residual deficit could be predicted most accurately by the degree of the subacute deficit.
51 When using imaging parameters for the prediction of the residual deficit, including
52 information about the lesion topology increased prediction accuracy. A subset of anatomical
53 regions within the ischemic lesion had particular impact on the prediction of long-term
54 outcome. Prediction accuracy depended on the degree of functional impairment.

55 **Conclusions:** For the first time, we identified and characterized predictors of post-stroke
56 outcome in a large cohort of mice and found strong concordance with clinical data. These
57 results are discussed in light of study design and imaging limitations. In the future, using
58 outcome prediction can improve the design of preclinical studies and guide intervention
59 decisions.

61 **NON-STANDARD ABBREVIATIONS AND ACRONYMS**

62 **AMBA** Allen Mouse Brain Atlas
63 **CCA** Common Carotid Artery
64 **ECA** External Carotid Artery
65 **FOV** Field Of View
66 **ICA** Internal Carotid Artery
67 **IQR** Interquartile Range
68 **LSMD** Least Square Mean Difference
69 **MD** Mean difference
70 **MCA** Middle Cerebral Artery
71 **MCAO** Middle Cerebral Artery Occlusion
72 **MedAE** Median Absolute Error
73 **PA** Pterygopalatine Artery
74 **pp** percentage points
75 **PE** prediction error

77 **Keywords**

78 stroke, mice, outcome prediction, motor-function, staircase

79 INTRODUCTION

80 Stroke remains a major public health challenge, as its occurrence rises in aging societies.¹
 81 With decreasing mortality rates due to progress in acute stroke therapy, the need to develop
 82 treatments that improve functional outcome has become more pressing.² Understanding
 83 predictors of functional outcome after stroke both in humans and rodents is an essential step
 84 towards defining adequate treatment decisions and improving the design of preclinical
 85 studies.³ Prediction of expected motor-functional outcomes in mice could potentially guide
 86 researchers in their treatment decisions in preclinical stroke intervention studies and support
 87 outcome-dependent stratifications. In humans, magnetic resonance imaging (MRI) is used to
 88 assess stroke volume and topology.⁴ Lesion volume is most commonly used to analyze stroke
 89 severity and predict functional outcome, but the prognostic value has been shown to be better
 90 when including lesion topology.⁵⁻¹¹ This was also shown in an exploratory preclinical study
 91 using a porcine stroke model.¹² Additionally, the degree of the subacute deficit has been
 92 shown to be a reliable predictor of long-term outcome, especially for mild functional
 93 deficits.^{13,14} In contrast to humans, little is known about predictors of functional outcome after
 94 stroke in mice, although they are commonly used in preclinical research. The stroke
 95 preclinical assessment network, for instance, recently completed the largest preclinical stroke
 96 study on mice and provided examples of how the middle cerebral artery occlusion (MCAO)
 97 model can be used to conduct studies that are similar to those performed in humans.¹⁵
 98 Although highly standardized procedures such as the filamentous MCAO have been
 99 developed in rodent stroke research, lesion volume and topology differ between individual
 100 mice, for instance, because of variations in the vasculature and degree of collaterals, such as
 101 the patency of the posterior communicating artery.¹⁶ In addition, lesion volumes are different
 102 between mouse strains.¹⁷ Due to the resulting variance of lesion volumes and topology as well
 103 as small sample sizes in rodent stroke research, a systematic analysis of predictors of post-
 104 stroke outcome using early non-invasive MRI is challenging. Furthermore, detecting motor-
 105 functional deficits in rodents following stroke is difficult as they show impressive recovery
 106 and have subtle, if any, long-term motor deficits in common behavioral tests.¹⁸
 107 In a previous study, we have investigated accuracy of early perfusion/diffusion MRI for final
 108 infarct prediction.¹⁹ The main goal of the present study was to identify and compare different
 109 predictors of functional outcome following brain ischemia in mice. We therefore aggregated
 110 imaging and behavioral data from 13 MCAO studies. Using a newly modified protocol for the
 111 staircase test of skilled reaching, we tested forepaw function before and after stroke over a
 112 period of 41 days. We defined two phases of post-stroke recovery and tried to predict
 113 functional outcome after one week (subacute outcome) or three weeks (long-term outcome)
 114 using early MRI. We hypothesized that incorporating lesion topology and behavioral data
 115 would improve the predictability of post-stroke outcomes compared to using only the lesion
 116 volume. Therefore, we compared the prognostic value of lesion volume and topology for
 117 predicting the *subacute deficit* and additionally included the *subacute deficit* for predicting the
 118 *residual deficit* using machine learning on a large cohort of 148 mice. We replicated our
 119 findings in an independent cohort. Our work opens new avenues towards a better
 120 understanding of post-stroke recovery and impairment in mice and paves the way to using
 121 prediction of functional outcome for the optimization of preclinical stroke studies.

122

METHODS

Experimental Design

13 studies from 2016 to 2019 were pooled for behavioral and imaging analyses. Mice were trained in the staircase test for three weeks before and after 45 min of MCAO surgery followed by MRI after 24 hours (Figure 1A, details in Supplemental Materials & Methods). 360 mice were considered for inclusion into this study. Four exclusion criteria were pre-specified (Figure S1): **1)** In the third week of testing, mice performed below 20% of the average in the staircase test (n=30); **2)** no visible infarct in MRI (n=18); **3)** Surgical death or humane euthanasia before study end (n=121) and **4)** incomplete data sets for behavioral data (n=25). Following these criteria, 166 mice were included (Table S1). To validate our prediction models, an additional cohort was built, termed *replication cohort*, using two studies from 2015 and 2019 with n=49 mice finally included (Figure S2). Basic characteristics of the animals are provided in Table S2 and Figure S3.

Staircase Test of Skilled Reaching

Behavioral testers were blinded to the intervention and MRI results. Mice were housed, food restricted and familiarized with the staircase test (details in Supplemental Materials & Methods).²⁰ We chose one experimental variable, the percentage of collected pellets per side. Performance was expressed as a percentage of average pre-stroke performance (*baseline*). Mice were randomized and allocated to either MCAO or sham surgery. Based on the mean performance of the entire cohort after stroke, two phases were defined: a '*subacute deficit*' phase (days 2–6), during which performance appeared dynamic and increasing, and a '*residual deficit*' phase (days 12–21), throughout which performance appeared stable. Average performance was calculated for each mouse for the respective period. A gap of five days was chosen between the *subacute* and *residual deficit* to ensure the dynamic phase had ended.

Classification of Severity Grades for Subgroup Analysis

Alluding to the modified Rankin scale, a score regularly used in stroke patients, five different functional subgroups were defined.²¹ Subgroups were based on the severity of the motor-functional deficit of the paretic paw: mild (performance >80%), moderate-mild (60–79%), moderate (40–59%), moderate-severe (20–39%) and severe deficit (0–19%). Both *subacute* and *residual deficit* were used to define subgroups, depending on the analysis context (Figure 1B–D).

Selection of Predictors

Two factors were analyzed for their predictive value for the degree of the *subacute deficit* after MCAO: **1)** stroke *lesion volume* measured within the coordinates of the Allen Mouse Brain Atlas (AMBA), which makes it identical to the volume of remaining brain tissue,²² and **2)** MRI lesion percentages measured in the 736 AMBA regions. Throughout the manuscript, this predictor is referred to as *segmented MRI*. The dimensionality of the *segmented MRI* (736 initial regions) was reduced by discarding all regions that did not show a lesion in at least one animal. This left the *segmented MRI* with 536 regions. In addition to those two imaging-based parameters, for the prediction of the *residual deficit*, the degree of *subacute deficit* was included as a third factor.

Development of Prediction Models with Machine Learning

For development of machine learning based prediction models, we divided the data set into a training (2/3 of the animals) and a test (1/3 of the animals) group (details in Supplemental Materials & Methods). For each predictor, we calculated the median absolute error (MedAE) and report the average as *prediction error (PE)*. Only *PEs* from the test cohort were used for accuracy analysis. *PE* measures the difference between predicted and actual performance. Small errors indicate high accuracy. First and third quartiles and interquartile ranges (IQR) of absolute error were calculated to estimate *PE* variation within a cohort. To determine which anatomical regions affect MRI-based *residual deficit* prediction accuracy, the *out-of-bag* predictor importance for each anatomical region in the *segmented MRI* was calculated (details in Supplemental Materials & Methods).²³

Statistics, Data Availability & Ethics Approval

Data are reported according to the ARRIVE guidelines. Methods for statistics, data display and availability including ethics approval are described in the Supplemental Materials & Methods.

RESULTS

MRI Characterization and Lesion Topology

Total cohort and functional subgroup incidence maps were generated (Figure 2A). Average *lesion volume* was 25.00 mm³ (95% CI: 21.46–28.54). While heterogeneity of stroke volumes was increased in the 45 minutes compared to a 30 minutes occlusion (Figure S4), it was smaller than in a previously published study performing 60 minutes of MCA occlusion.¹⁵ Classified by degree of residual deficit, mean lesion volume was 14.03 mm³ (9.82–18.25) in mild, 17.17 mm³ (12.52–21.82) in moderate to mild, 26.29 mm³ (16.86–35.73) in moderate, 33.62 mm³ (24.04–43.20) in moderate to severe, and 47.23 mm³ (36.79–57.68) in severe residual deficit mice (Figure 2B). One-Way ANOVA showed a significant difference in mean lesion volumes between functional subgroups ($F(4,143)=14.14$, $p<0.0001$; full report in Table S3). T2-weighted MR-images were co-registered on the AMBA to evaluate lesion topology (*segmented MRI*). Quantitative evaluation of the hyperintense lesion was performed on 536 regions and lesion volume in each region was expressed in percent (Table S4).

A Modified Staircase Test Can Assess Early and Long-Term Functional Outcome in Mice after Stroke

Performance peaked after approximately 7 days (Figure 3A–B). The average percentage of retrieved pellets during *baseline* testing was 49.26% (47.22–51.31) on the left (later non-paretic) side and 46.29% (44.16–48.42) on the right (later paretic) side in the MCAO group and 45.81% (37.38–54.23) and 47.11% (38.95–55.26) on the left and right sides in the sham group (Figure S5). Mixed effects analysis showed no side-group interaction ($F(1,164)=1.464$, $p=0.2281$). After MCAO, mean subacute performance was 61.60% (56.12–67.08) on the non-paretic side and 37.59% (31.92–43.26) on the paretic side (Figure 3C). In sham animals, subacute performance was 78.40% (63.46–93.34) on the left and 72.23 (57.30–87.15) on the right side. Mixed-effects analysis found a significant interaction between side and group ($F(1,164)=4.189$, $p=0.0423$). After correcting for multiple comparisons using Šidák's test, MCAO animals had significantly lower paretic paw performance than sham (LSMD=34.63 percentage points [pp], $t=4.092$, $DF=328$, $p=0.0001$). After correcting for multiple comparisons using Šidák's test, performance of the paretic paw was significantly lower in MCAO animals when compared to sham (LSMD=34.63pp, $t=4.092$, $DF=328$, $p=0.0001$). Non-paretic sides did not differ between groups (LSMD=16.80pp, $t=1.985$, $DF=328$, $p=0.0937$). Paired t-test was performed to test for a difference in between paretic and non-paretic paws of the MCAO mice to show side-specificity of the motor-functional deficit. Performance in the paretic paw was significantly lower than in the non-paretic paw (MD: 24.01 %, 18.34–29.68, $t=8.365$, $df=147$, $p<0.0001$) (Figure S6A).

In the period of residual deficit, non-paretic performance was 95.35 % (89.54–101.17) and paretic performance was 60.88 % (54.94–66.81; Figure 3D). During the phase of residual deficit, sham animals performed 92.39% (81.80–102.98) on the non-paretic side and 91.56% (78.45–104.66) on the paretic side. Mixed-effects analysis showed a significant interaction between side and group ($F(1,164)=9.384$, $p=0.0026$). Using Šidák's test, paretic paw performance was significantly lower in MCAO animals compared to sham (LSMD=30.68pp, $t=3.501$, $DF=328$, $p=0.0011$). Non-paretic sides showed no statistically significant difference between groups (LSMD=2.96pp, $t=0.3377$, $DF=328$, $p=0.9302$). Finally, we analyzed the effects of the general well-being of the animals on functional outcome. We used the Modified

DeSimoni Neuroscore for the assessment of general deficits and the weight loss on day 2 as proxies for general well-being and found poor correlation to the degree of either subacute or residual deficit (Figure S7 and S8).²⁴ In addition, *PEs* of weight loss or neuroscore were significantly higher compared to imaging- or performance-based prediction (Figure S9 and S10).

Prediction of Subacute Deficit from Acute MR Imaging

Using random forest and early non-invasive MRI data, *subacute deficit* prediction models were created. *PE* was 13.30pp (13.00–13.59, *Q*₁: 5.98, *Q*₃: 31.48, IQR: 25.51) for the *lesion volume* and 16.23pp (16.03–16.42, *Q*₁: 8.04, *Q*₃: 29.18, IQR: 21.14) for the *segmented MRI* (Figure 4A–B). Unpaired, two-tailed t-test revealed, that *PE* was significantly smaller when using the *lesion volume* as a predictor compared to the *segmented MRI* (MD=2.93pp, 2.58–3.28, *t*=16.60, *df*=98, *p*<0.0001).

Prediction of Residual Deficit from Subacute Deficit and MRI

PE was 18.90pp (18.70–19.09, *Q*₁: 8.04, *Q*₃: 29.09, IQR: 21.05) for the *subacute deficit*, 22.68pp (22.46–22.90, *Q*₁: 14.07, *Q*₃: 41.84, IQR: 27.77) for the *segmented MRI* and 25.95pp (25.71–26.29, *Q*₁: 12.21, *Q*₃: 41.25, IQR: 29.04) for the *lesion volume* (Figure 4C–D). One-way ANOVA showed predictors differed significantly (*F*(2,147)=1032, *p*<0.0001). After multiple comparisons were corrected using Tukey's test, the *PE* of the *subacute deficit* was significantly smaller than *PE* of the *segmented MRI* (MD=3.79pp, 4.15–3.42, *p*<0.0001) and the *lesion volume* (MD=7.06pp, 7.43–6.69, *p*<0.0001). *Segmented MRI* outperformed the prediction accuracy of the *lesion volume* (MD=3.28pp, 3.65–2.91, *p*<0.0001).

Identification of Anatomical Regions Associated with Long-Term Outcome

To better understand which anatomical regions within the lesion best predict long-term outcome, the contribution of each region measured by MRI was analyzed by quantifying its importance within the random forest algorithm. We found 81 regions with above-zero out-of-bag predictor importance, meaning they contribute more than random data (Figure 5A–B, Table S5). Among those regions were the caudoputamen, the primary somatosensory area, the external capsule and the corticospinal tract. In the next step, random forest models were trained using increasing number of MRI regions, starting with the most important region. The *PE* of those models gradually decreased with increasing number of MRI regions (Figure 5C). *PE* quickly reached a plateau, and adding more regions only slightly improved accuracy. A relevant local minimum of *PE* was observed with the first 14 anatomical regions (*PE*=22.91pp).

Validation in an Independent Cohort

As a final step, we tested our prediction models on the independent *replication cohort*. Imaging and behavioral analyses can be found in the Supplemental Materials & Methods. For the prediction of the *subacute deficit*, mean *PE* when using the *lesion volume* was 23.19pp (22.85–23.53) and 20.00pp (19.74–20.27) for the *segmented MRI* (Figure 6A–B). In contrast to our first cohort, now the *segmented MRI* provided significantly smaller *PEs* compared to the *lesion volume* (MD=3.19pp, 3.61–2.76, *t*=14.89, *df*=98, *p*<0.0001). The *PE* for the *residual deficit* using the *subacute deficit* was 10.76pp (10.31–11.22), 22.96pp (22.15–23.77) for the *segmented MRI* and 23.94pp (23.41–24.46) for the *lesion volume* (Figure 6C–D). One-

way ANOVA revealed, that there was a statistically significant difference between predictors ($F(2,147)=18.98$, $p<0.0001$). After correction for multiple comparisons using Tukey's test, the *PE* of the *subacute deficit* was significantly smaller than the *PE* of the *segmented MRI* ($MD=12.20pp$, $13.23-11.17$, $p<0.0001$) and the *lesion volume* ($MD=13.18pp$, $14.20-12.15$, $p<0.0001$). The difference between *segmented MRI* and the *lesion volume* was less clear than in our first cohort, but trended towards significance, with the *segmented MRI* providing slightly smaller *PEs* compared to the *lesion volume* ($MD=0.98pp$, $2.01-0.05$, $p=0.0668$). Lastly, we tested the prediction accuracy when including an increasing number of anatomical regions. Only regions we identified to have an impact on the prediction of the *residual deficit* in our *testing cohort* were used. Surprisingly, in our *replication cohort*, using the lesion percentage in the caudoputamen provided smaller *PEs* compared to using the entire *segmented MRI* or the *lesion volume*. When adding an increasing number of regions, we first observed a sharp spike in *PEs*, followed by a slow decrease. Excitingly, after including fourteen regions, we again observed a local minimum of *PE* (Figure 6E), replicating our finding from the *testing cohort*.

DISCUSSION

In this study, we systematically compared different predictors of subacute and long-term functional outcomes after stroke in a large cohort of mice. We used MRI derived parameters such as the *lesion volume* and *lesion topology*, as well as early functional testing to predict post-stroke performance in a pellet reaching task. Studies with large sample sizes have transformed preclinical MRI research and corresponding open data repositories have proven extremely valuable, e.g. in the context of robust functional networks measured by resting state fMRI.²⁵ Predictors of post-stroke outcome, such as imaging-derived parameters or functional data, have previously been extensively studied in humans.^{2-6,8} While one preclinical study on predictors of stroke outcome in a porcine MCAO model exists, evidence on prediction of stroke outcome in mice is scarce, despite rodents being used most commonly as model animals in stroke studies.^{12,26}

Using a modified protocol for the staircase test of skilled reaching in mice, we were able to monitor motor function daily and to detect both subacute and long-term functional deficits.^{20,27} A side-specific disability of the forepaw was detected over three weeks post-surgery. This indicates that performance was governed by the stroke and not by general sickness behavior. We observed distinct trajectories of functional recovery. The differentiation between recoverees and non-recoverees is comparable to what can be observed in humans.¹⁴ The resemblance to the human recovery process supports the predictive value of stroke modeling in mice and the case for implementing sophisticated behavioral tests that involve a longer phase of training prior to stroke for assessing long-term impairments.²⁸ For future applications, one has to consider the possible impact of food restriction included as part of the staircase training and testing on mortality and lesion volume.²⁹

The *lesion volume* was the best predictor for the *subacute deficit* after stroke in mice as measured by *PE* in our *testing cohort*. In the *replication cohort* it was outperformed by the *segmented MRI*, which included information about the lesion topology. While *PEs* remained low, this is clearly a difference between the two cohorts. However, we also observed differences in stroke size and topology between the two cohorts. In our *replication cohort* lesion volumes were bigger and cortical regions accounted for higher proportions of the *lesion volume* compared to the *testing cohort*. While it has previously been stated that lesion volume functions as a good predictor for acute stroke outcome, our data suggests that in mice with greater cortical lesions taking into account topological information provides a more accurate prediction of early functional outcome.⁶ For the long-term motor-functional outcome, in the *testing cohort* the *segmented MRI* provided significantly better prediction accuracies than the *lesion volume*. This indicates that for functional recovery, lesion topology is more relevant than lesion volume, which again is in line with clinical data.^{11,12} It should be noted, that in the 45 min MCAO model, lesion volume and lesion topology are not fully independent predictors. Larger ischemic lesions typically include cortical regions while smaller lesions are restricted to subcortical structures. This phenomenon can be observed in the results of our *replication cohort*, where the difference between the *segmented MRI* and the *lesion volume* was only marginal but trending towards significance.

Following up on the influence of lesion topology, we identified anatomical regions that drive imaging-based prediction of the *residual deficit*. We found that considering only a subset of anatomical regions can explain functional long-term outcome. Prediction accuracy displayed a local maximum after 14 regions had been added to the prediction model. Among those regions were both, cortical and subcortical regions typically affected by a MCAO stroke such

as the caudoputamen and the primary somatosensory area. Evidently, the caudoputamen is damaged and part of the lesion core in the transient occlusion model but also serves as the structure that best predicts the performance. Further, white matter regions such as the corpus callosum and the fiber tracts showed to be of particular importance for the prediction of long-term outcome. This is in line with previous studies in humans suggesting that lesions of the corticospinal tract seem to be more important to both early and long-term functional outcome than lesion volume.^{30,31} These findings could be replicated in our independent *replication cohort*, where a local minimum of *PE* could be observed after including the same 14 regions. Again, lesions in the caudoputamen had a major impact on prediction accuracies, outperforming both cortical grey and white matter structures.

Imaging-based predictors offered good estimates of post-stroke long-term outcome but the best predictor of the *residual deficit* was the degree of the *subacute deficit*, again confirming studies on predictors of post-stroke outcome in humans.³² Lastly, we found that independent of the chosen model, the prediction accuracy for both the *subacute* and *residual deficits* depended on the degree of the deficit. In line with clinical data, we found that severe *residual deficits* are more difficult to predict than moderate-to-mild deficits.^{13,14}

Study Limitations

We have restricted our prediction tools to 45 min of MCAO using endoluminal filament occlusion. As the data was pooled from 13+2 studies performed between 2015 and 2019, the dataset contained various co-variates. However, variance analysis revealed that sex, genotype, surgeon, or age did not significantly explain differences in performance after stroke. We cannot exclude confounding effects of housing, lab chow diet, anesthesia, or further co-variates. Furthermore, we did not replicate our results with other behavioral readouts than the staircase test of skilled pellet reaching. Additionally, using MR imaging from a later time point, e.g. 21 days after MCAO, would have likely resulted in even better prediction accuracies. However, prediction of functional outcome that is based on late MR-imaging cannot be used for guiding intervention decisions in future preclinical studies as the window of opportunity in mice has proven to be narrow.³³ Another limitation of our approach is the manual delineation of lesion masks. Although manual lesion segmentation is still the gold standard today, well-documented, multi-centric and openly available stroke T1-weighted MRI datasets pave the way towards fully automated algorithms for MRI stroke lesion segmentation in humans.³⁴⁻³⁶ Results from T2-weighted MRI in rodent stroke models are also promising with excellent similarity between manual segmentation and fully automated algorithms exceeding agreement between multiple raters.^{37,38} These studies have facilitated significant progress in the pursue to fully automate lesion segmentation.^{38,39} Nulling of the fluid signal via e.g. FLAIR MRI could have improved the discrimination between CSF and ischemic lesion. However, 24 hours after MCAO, CSF has still higher signal on RARE than the lesion and the walls of the lateral ventricles can be reliably identified.²² For later time points, an adjusted imaging protocol might have to be applied. Animals' unspecific sickness behavior during the *subacute deficit* phase may have contributed to the degree of performance loss. The differences between sham and MCAO, as well as paretic and non-paretic paw, were, however, significant, indicating that our behavioral paradigm detects stroke-specific motor-functional deficits. There were no video recordings of the testing sessions to account for differences in kinematics but the entire behavioral data set has been uploaded in the repository linked to this study. Analysis of lesion volumes stratified by functional subgroups might be partly

weakened by experimental bias, since lesion volume and performance are strongly correlating. Finally, we corrected only for multiple tests in a single test set and not for multiple comparisons between different tests or hypotheses.

CONCLUSIONS

In conclusion, we have here for the first time identified and characterized predictors of post-stroke outcome in mice. The concordance with clinical data strengthens the usability of mice as model animals in preclinical studies. Prediction of outcome in intervention studies using non-invasive MRI measurements or motor-functional data should be utilized to compare expected and achieved motor-function outcomes, select mice with particularly poor predicted outcomes, and guide treatment or intervention options. This will help to improve the reproducibility of preclinical rodent stroke research and close the translational gap.

Acknowledgments

Janet Lips coordinated experiments and contributed with MRI, handling, and behavioral evaluation; Larissa Mosch (behavior, histology), Monika Dopatka (surgeries), and Marco Foddis (surgeries, behavioral assessment, and MRI) all provided excellent technical assistance. Figures were created with biorender.com

Sources of Funding

Funding was provided by the Deutsche Forschungsgemeinschaft (DFG, German Research Foundation) to C.J.H. and C.H. (Project number 417284923), to P.B.S. (Project number 428869206), to N.W., M.E., and C.H. (Project number 424778381–TRR 295) and NeuroCure (EXC–2049–390688087) and the German Federal Ministry of Education and Research (BMBF, Center for Stroke Research Berlin 01EO1301) to U.D., P.B.S., and C.H., and to P.B.S. by the BMBF under the ERA-NET NEURON scheme (01EW1811). M.Ku. received funding from the DFG Graduate School 203. This work was supported by Charité^{3R} Replace–Reduce–Refine and partly by the Fondation Leducq to M.E., and C.H.. F.K. and M.Eg. received a scholarship from the Berlin Institute of Health, Berlin. P.E., N.W., and C.J.H. are participants in the Charité Clinical Scientist Program funded by the Charité – Universitätsmedizin Berlin and the Berlin Institute of Health and N.W. is a Freigeist Fellow with support from the Volkswagen Foundation. In addition, this work was supported by DFG (Project number 73500270 and 413848220) and ERA-NET NEURON EBio2, with funds from BMBF 01EW2004 to J.P.D.

Disclosures

All authors certify that they have no affiliations with or involvement in any organization or entity with any financial interest or non-financial interest in the subject matter or materials discussed in this manuscript. No funding was received to assist with the preparation of this manuscript.

Supplemental Materials & Methods

Checklist

Expanded Materials & Methods

Online Figures S1-S13

Tables S1-8

References

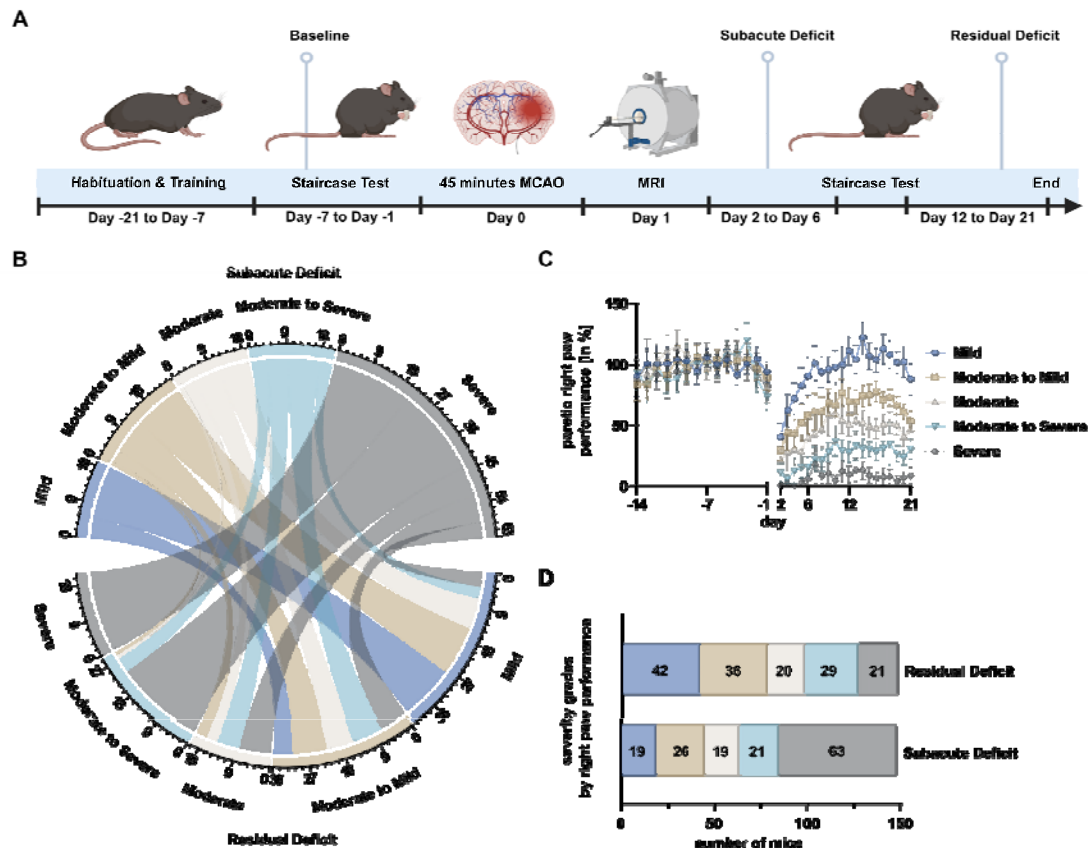
1. Béjot Y, Bailly H, Durier J, Giroud M. Epidemiology of stroke in Europe and trends for the 21st century. *Press. Medicale*. 2016;45:e391–e398. doi:10.1016/j.lpm.2016.10.003
2. Eriksson M, Norrving B, Terént A, Stegmayr B. Functional Outcome 3 Months after Stroke Predicts Long-Term Survival. *Cerebrovasc. Dis.* 2008;25:423–429. doi:10.1159/000121343
3. Farr TD, Wegener S. Use of magnetic resonance imaging to predict outcome after stroke: A review of experimental and clinical evidence. *J. Cereb. Blood Flow Metab.* 2010;30:703–717. doi:10.1038/jcbfm.2010.5
4. Albers GW, Thijs VN, Wechsler L, Kemp S, Schlaug G, Skalabrin E, Bammer R, Kakuda W, Lansberg MG, Shuaib A, et al. Magnetic resonance imaging profiles predict clinical response to early reperfusion: The diffusion and perfusion imaging evaluation for understanding stroke evolution (DEFUSE) study. *Ann. Neurol.* 2006;60:508–517. doi:10.1002/ana.20976
5. Schiemanck SK, Post MWM, Kwakkel G, Witkamp TD, Kappelle LJ, Prevo AJH. Ischemic lesion volume correlates with long-term functional outcome and quality of life of middle cerebral artery stroke survivors. *Restor. Neurol. Neurosci.* 2005;23:257–263.
6. Lövblad KO, Baird AE, Schlaug G, Benfield A, Siewert B, Voetsch B, Connor A, Burzynski C, Edelman RR, Warach S. Ischemic lesion volumes in acute stroke by diffusion-weighted magnetic resonance imaging correlate with clinical outcome. *Ann. Neurol.* 1997;42:164–170. doi:10.1002/ana.410420206
7. Pinto A, McKinley R, Alves V, Wiest R, Silva CA, Reyes M. Stroke lesion outcome prediction based on MRI imaging combined with clinical information. *Front. Neurol.* 2018;9:1–10. doi:10.3389/fneur.2018.01060
8. Cheng B, Forkert ND, Zavaglia M, Hilgetag CC, Golsari A, Siemonsen S, Fiehler J, Pedraza S, Puig J, Cho TH, et al. Influence of stroke infarct location on functional outcome measured by the modified rankin scale. *Stroke*. 2014;45:1695–1702. doi:10.1161/STROKEAHA.114.005152
9. Borich MR, Brodie SM, Gray WA, Ionta S, Boyd LA. Understanding the role of the primary somatosensory cortex: Opportunities for rehabilitation. *Neuropsychologia*. 2015;79:246–255. doi:10.1016/j.neuropsychologia.2015.07.007
10. Munsch F, Sagnier S, Asselineau J, Bigourdan A, Guttmann CR, Debruxelles S, Poli M, Renou P, Perez P, Dousset V, et al. Stroke location is an independent predictor of cognitive outcome. *Stroke*. 2016;47:66–73. doi:10.1161/STROKEAHA.115.011242
11. Menezes NM, Ay H, Zhu MW, Lopez CJ, Singhal AB, Karonen JO, Aronen HJ, Liu Y, Nuutinen J, Koroshetz WJ, et al. The real estate factor: Quantifying the impact of infarct location on stroke severity. *Stroke*. 2007;38:194–197. doi:10.1161/01.STR.0000251792.76080.45
12. Scheulin KM, Jurgielewicz BJ, Spellicy SE, Waters ES, Baker EW, Kinder HA, Simchick GA, Sneed SE, Grimes JA, Zhao Q, et al. Exploring the predictive value of lesion topology on motor function outcomes in a porcine ischemic stroke model. *Sci. Rep.* 2021;11:1–15. doi:10.1038/s41598-021-83432-5
13. Zarahn E, Alon L, Ryan SL, Lazar RM, Vry MS, Weiller C, Marshall RS, Krakauer JW. Prediction of motor recovery using initial impairment and fMRI 48 h poststroke.

- 45 *Cereb. Cortex.* 2011;21:2712–2721. doi:10.1093/cercor/bhr047
- 46 14. Vliet R, Selles RW, Andrinopoulou E, Nijland R, Ribbers GM, Frens MA, Meskers C,
47 Kwakkel G. Predicting Upper Limb Motor Impairment Recovery after Stroke: A
48 Mixture Model. *Ann. Neurol.* 2020;87:383–393. doi:10.1002/ana.25679
- 49 15. Lyden PD, Bosetti F, Diniz MA, Rogatko A, Koenig JI, Lamb J, Nagarkatti KA,
50 Cabeen RP, Hess DC, Kamat PK, et al. The Stroke Preclinical Assessment Network:
51 Rationale, Design, Feasibility, and Stage 1 Results. *Stroke.* 2022;53:1802–1812.
52 doi:10.1161/STROKEAHA.121.038047
- 53 16. Knauss S, Albrecht C, Dirnagl U, Mueller S, Harms C, Hoffmann CJ, Koch SP, Endres
54 M, Boehm-Sturm P. A Semiquantitative Non-invasive Measurement of PcomA Patency
55 in C57BL/6 Mice Explains Variance in Ischemic Brain Damage in Filament MCAo.
56 *Front. Neurosci.* 2020;14:1–11. doi:10.3389/fnins.2020.576741
- 57 17. Maeda K, Hata R, Hossmann KA. Differences in the cerebrovascular anatomy of
58 C57Black/6 and SV129 mice. *Neuroreport.* 1998;9:1317–1319. doi:10.1097/00001756-
59 199805110-00012
- 60 18. Weber RZ, Mulders G, Kaiser J, Tackenberg C, Rust R. Deep learning based behavioral
61 profiling of rodent stroke recovery. *bioRxiv.* 2021;
- 62 19. Leithner C, Füchtmeier M, Jorks D, Mueller S, Dirnagl U, Rojl G. Infarct Volume
63 Prediction by Early Magnetic Resonance Imaging in a Murine Stroke Model Depends
64 on Ischemia Duration and Time of Imaging. *Stroke.* 2015;46:3249–3259.
65 doi:10.1161/STROKEAHA.114.007832
- 66 20. Baird AL, Meldrum A, Dunnett SB. The staircase test of skilled reaching in mice. *Brain*
67 *Res. Bull.* 2001;54:243–250. doi:10.1016/S0361-9230(00)00457-3
- 68 21. Bamford JM, Sandercock PAG, Warlow CP, Slattery J. Interobserver agreement for the
69 assessment of handicap in stroke patients: To the editor. *Stroke.* 1989;20:828.
70 doi:10.1161/01.STR.20.6.828
- 71 22. Koch S, Mueller S, Foddis M, Bienert T, von Elverfeldt D, Knab F, Farr TD, Bernard
72 R, Dopatka M, Rex A, et al. Atlas registration for edema-corrected MRI lesion volume
73 in mouse stroke models. *J. Cereb. Blood Flow Metab.* 2019;39:313–323.
74 doi:10.1177/0271678X17726635
- 75 23. Breiman L. Random Forests. *Mach. Learn.* 2001;45:5–32.
76 doi:10.1023/A:1010933404324
- 77 24. Donath S, An J, Lee SLL, Gertz K, Datwyler AL, Harms U, Müller S, Farr TD,
78 Füchtmeier M, Lättig-Tünnemann G, et al. Interaction of ARC and DAXX: A novel
79 endogenous target to preserve motor function and cell loss after focal brain ischemia in
80 mice. *J. Neurosci.* 2016;36:8132–8148. doi:10.1523/JNEUROSCI.4428-15.2016
- 81 25. Grandjean J, Canella C, Anckaerts C, Ayrancı G, Bougacha S, Bienert T, Buehlmann
82 D, Coletta L, Gallino D, Gass N, et al. Common functional networks in the mouse brain
83 revealed by multi-centre resting-state fMRI analysis. *Neuroimage.* 2020;205.
84 doi:10.1016/j.neuroimage.2019.116278
- 85 26. Casals JB, Pieri NCG, Feitosa MLT, Ercolin ACM, Roballo KCS, Barreto RSN,
86 Bressan FF, Martins DS, Miglino MA, Ambrósio CE. The use of animal models for
87 stroke research: a review. *Comp. Med.* 2011;61:305–13.

- 88 doi:10.1109/TAES.1968.5408692
- 89 27. Bravo-Ferrer I, Cuartero MI, Zarruk JG, Pradillo JM, Hurtado O, Romera VG, Díaz-
90 Alonso J, García-Segura JM, Guzmán M, Lizasoain I, et al. Cannabinoid type-2
91 receptor drives neurogenesis and improves functional outcome after stroke. *Stroke*.
92 2017;48:204–212. doi:10.1161/STROKEAHA.116.014793
- 93 28. Corbett D, Carmichael ST, Murphy TH, Jones TA, Schwab ME, Jolkonen J, Clarkson
94 AN, Dancause N, Wieloch T, Johansen-Berg H, et al. Enhancing the Alignment of the
95 Preclinical and Clinical Stroke Recovery Research Pipeline: Consensus-Based Core
96 Recommendations from the Stroke Recovery and Rehabilitation Roundtable
97 Translational Working Group □. *Neurorehabil. Neural Repair*. 2017;31:699–707.
98 doi:10.1177/1545968317724285
- 99 29. Manzanero S, Gelderblom M, Magnus T, Arumugam T V. Calorie restriction and
100 stroke. *Exp. Transl. Stroke Med*. 2011;3:1–13. doi:10.1186/2040-7378-3-8
- 101 30. Lindenberg R, Renga V, Zhu LL, Betzler F, Alsop D, Schlaug G. Structural integrity of
102 corticospinal motor fibers predicts motor impairment in chronic stroke. *Neurology*.
103 2010;74:280–287. doi:10.1212/WNL.0b013e3181ccc6d9
- 104 31. Feng W, Wang J, Chhatbar PY, Doughty C, Landsittel D, Lioutas V, Kautz SA,
105 Schlaug G. Corticospinal tract lesion load: An imaging biomarker for stroke motor
106 outcomes. *Ann. Neurol*. 2015;78:860–70. doi:10.1002/ana.24510
- 107 32. Frankel MR, Morgenstern LB, Kwiatkowski T, Lu M, Tilley BC, Broderick JP, Libman
108 R, Levine SR, Brott T. Predicting prognosis after stroke: A placebo group analysis from
109 the National Institute of Neurological Disorders and Stroke rt-PA stroke trial.
110 *Neurology*. 2000;55:952–959. doi:10.1212/WNL.55.7.952
- 111 33. Zeynalov E, Jones SM, Elliott JP. Therapeutic time window for conivaptan treatment
112 against stroke-evoked brain edema and blood-brain barrier disruption in mice. *PLoS*
113 *One*. 2017;12:1–8. doi:10.1371/journal.pone.0183985
- 114 34. Liew SL, Lo BP, Donnelly MR, Zavaliangos-Petropulu A, Jeong JN, Barisano G,
115 Hutton A, Simon JP, Juliano JM, Suri A, et al. A large, curated, open-source stroke
116 neuroimaging dataset to improve lesion segmentation algorithms. *Sci. Data*. 2022;9:1–
117 12. doi:10.1038/s41597-022-01401-7
- 118 35. Ito KL, Kim H, Liew SL. A comparison of automated lesion segmentation approaches
119 for chronic stroke T1-weighted MRI data. *Hum. Brain Mapp*. 2019;40:4669–4685.
120 doi:10.1002/hbm.24729
- 121 36. Verma K, Kumar S, Paydarfar D. Automatic Segmentation and Quantitative
122 Assessment of Stroke Lesions on MR Images. *Diagnostics*. 2022;12.
123 doi:10.3390/diagnostics12092055
- 124 37. Valverde JM, Shatillo A, De Feo R, Gröhn O, Sierra A, Tohka J. RatLesNetv2: A Fully
125 Convolutional Network for Rodent Brain Lesion Segmentation. *Front. Neurosci*.
126 2020;14:1–11. doi:10.3389/fnins.2020.610239
- 127 38. Mulder IA, Khmelinskii A, Dzyubachyk O, de Jong S, Rieff N, Wermer MJH, Hoehn
128 M, Lelieveldt BPF, van den Maagdenberg AMJM. Automated ischemic lesion
129 segmentation in MRI mouse brain data after transient middle cerebral artery occlusion.
130 *Front. Neuroinform*. 2017;11:1–15. doi:10.3389/fninf.2017.00003

39. An J, Wendt L, Wiese G, Herold T, Rzepka N, Mueller S, Koch SP, Hoffmann CJ, Harms C, Boehm-Sturm P. Deep learning-based automated lesion segmentation on mouse stroke magnetic resonance images. 2022; <https://www.biorxiv.org/content/10.1101/2022.08.09.503140v1>

136



137

Figure 1. Experimental design and assessment of functional subgroups

A, Mice were trained in pellet reaching for 21 days. Average percentage of retrieved pellets during the last week prior to MCAO was used to normalize performance (baseline). Mice received either 45 min of MCAO or sham surgery. MRI was performed on day 1 and mice were then tested for another 21 days. **B**, Chord diagram displaying the different trajectories of recovery. Groups on top display mice stratified by degree of *subacute deficit*, while groups on bottom display mice stratified by *residual deficit*. Numbers indicate group sizes. Interconnections visualize how many mice with a given *subacute deficit* recovered to have a given *residual deficit*, i.e. roughly a third of the mice with a severe *subacute deficit* displayed no recovery and showed a severe *residual deficit*. **C**, Performance of the paretic right paw over time for each severity grade. Error bars indicate 95% CI. Severity grades here were based on the degree of the *residual deficit*. **D**, Overview over sizes of functional subgroups. Groups are either based on the degree of *subacute* or *residual deficit*. While the majority of mice displayed a severe *subacute deficit*, due to their impressive capability for spontaneous recovery, the majority of mice displayed only mild *residual deficits*.

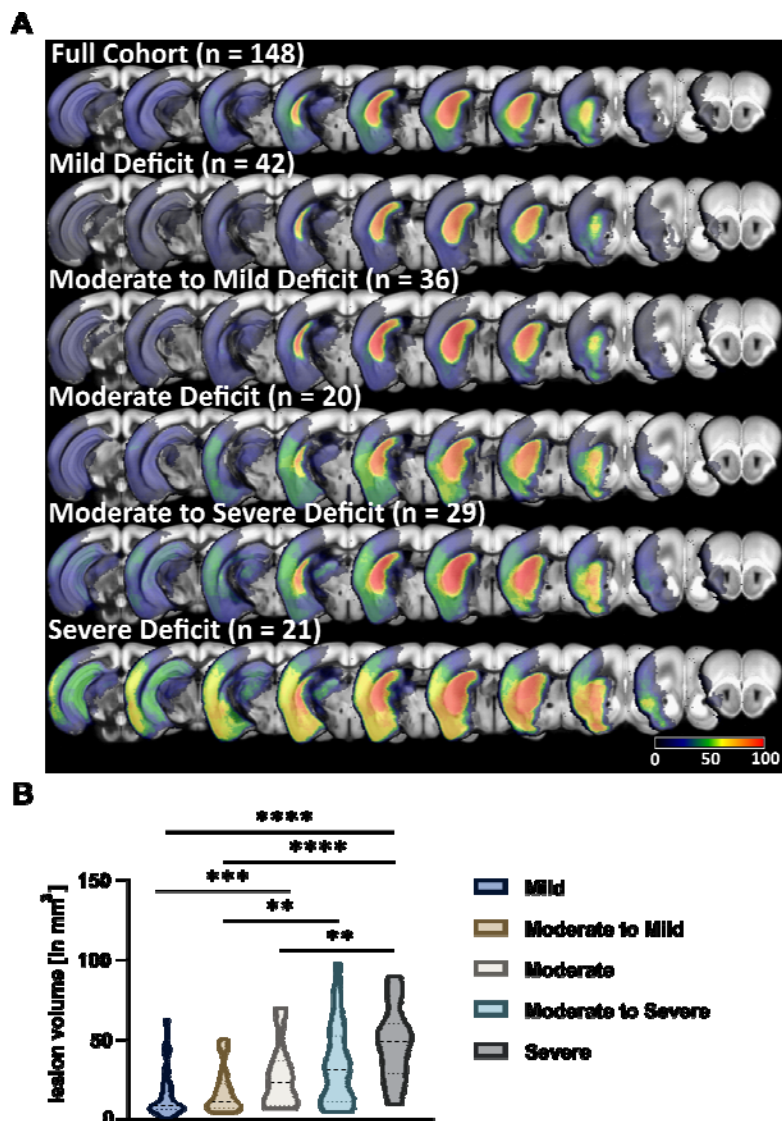


Figure 2. MRI characterization of lesion volume and location.

A, Coronal incidence maps of stroke lesions in the total cohort and the five different functional subgroups. Colours indicate percentage of mice with a lesion in a given region. Severity grades are based on degree of *residual deficit*. **B**, *lesion volume* by severity grade (based on degree of *residual deficit*). Great variability within functional subgroups could be observed and there was no significant difference when comparing *lesion volume* of consecutive severity grades, i.e. of mice with mild or moderate to mild *residual deficits*.

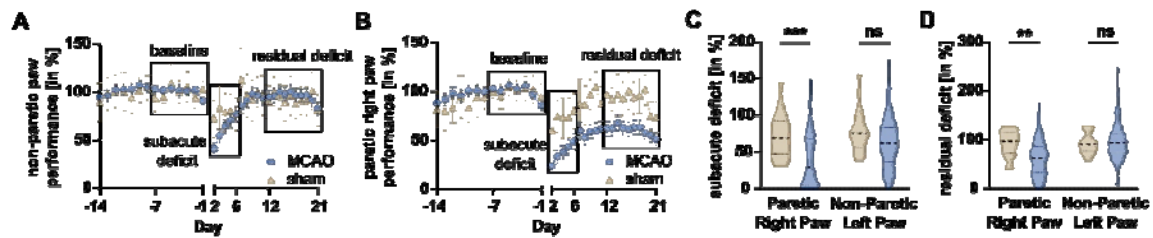


Figure 3. Assessing the sensorimotor deficit after stroke.

A, Non-paretic left and **B**, paretic right paw performance over time, bars depict 95% confidence interval. Performance on days -7 to -1 were averaged and taken as a baseline (first black rectangle). Data from days 2 to 6 were summarized and referred to as *subacute deficit* (second rectangle) while data from days 12 to 21 are referred to as *residual deficit* (third rectangle). **C**, *Subacute* and **D**, *residual deficit* of the non-paretic and paretic paw in sham (brown plot) and MCAO (blue plot) animals. Dashed lines indicate medians, dotted line indicate quartiles. Mixed-effects model followed by Šidák's post-hoc tests for multiple comparison were used to test effect of group and side.

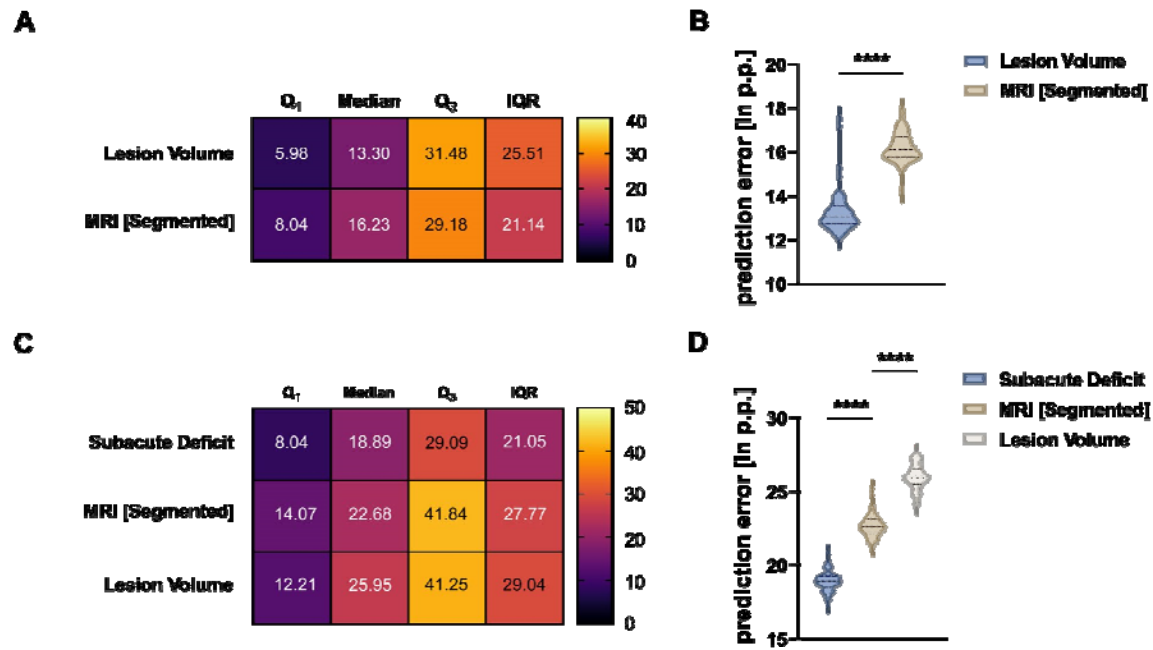


Figure 4. Comparison of predictors of the subacute and residual deficit.

A through **B**, Comparison of the prediction accuracy of the two predictors of the *subacute deficit*. Averaged Q₁, median, Q₃ and IQR were calculated using the 50 independent models for each predictor. Dashed lines indicate median, dotted lines indicate quartiles. Unpaired t-test was used to compare *PEs*. Small *PE* indicates small deviation between predicted and achieved performance. **C** through **D**, Comparison of prediction accuracy of the two imaging based parameters and the *subacute deficit* for the prediction of the *residual deficit*. Again, one-way ANOVA followed by Tukey's test for multiple comparison was used.

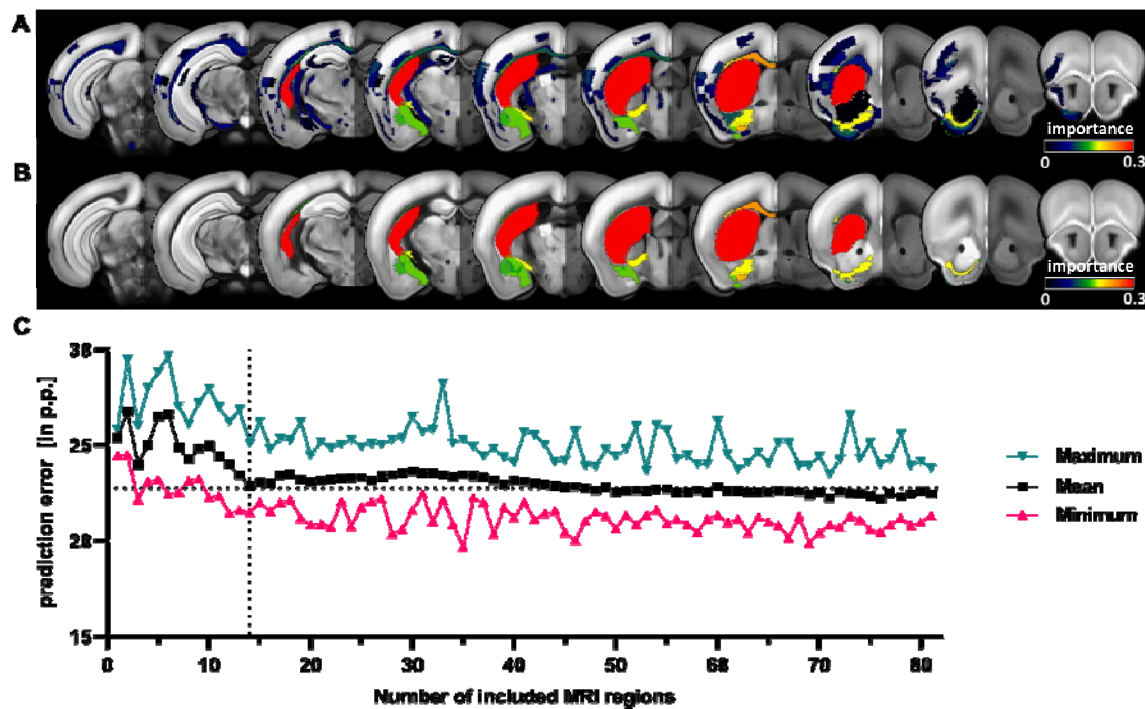


Figure 5. Identification of anatomical regions that drive imaging-based prediction of functional outcome.

A, Coronal slices depicting the importance of the 81 regions calculated from our random forest models (RF). Only regions with an importance level >0 are shown **B**, Visualization of the importance level of the 14 anatomical regions that were included in the prediction model that resulted in a local minimum of *PE*. **C**, Prediction of *residual deficit* was performed using an increasing number of regions in the *segmented MRI*. *PE* as well as maximum and minimum *PE* are depicted. Dashed lines at $x=14$ and $y=21.5$ denote the first local minimum of *PE* when including only 14 regions.

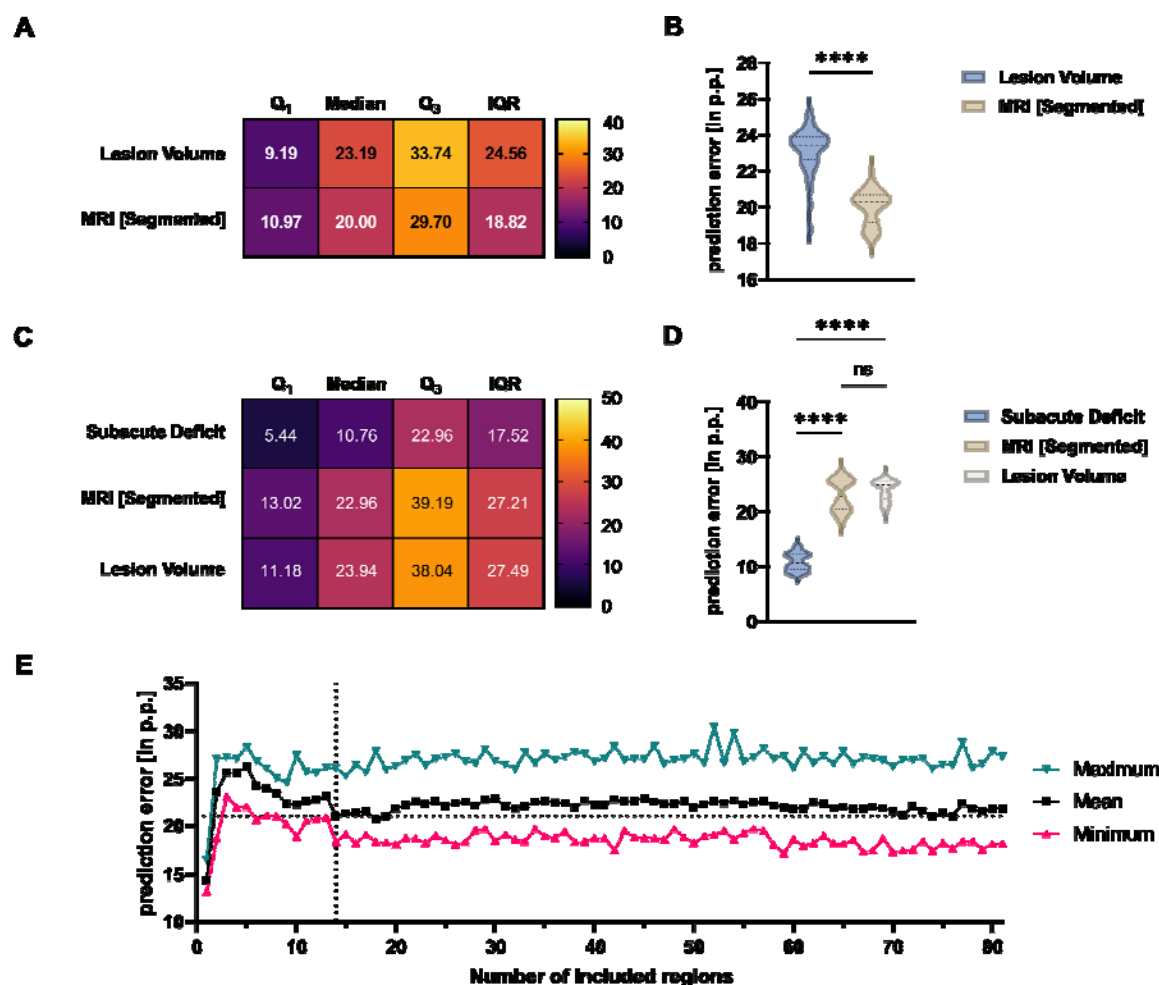


Figure 6. Validation of prediction models in an independent cohort.

A, through **B**, Comparison of the prediction accuracy of the two predictors of the *subacute deficit*. Dashed lines indicate median, dotted lines indicate quartiles. Unpaired t-test was used to compare *PEs*. While *PEs* were comparable to the ones seen in our testing cohort, subacute deficit was best predicted when using the segmented MRI **C** through **D**, Comparison of prediction accuracy of the two imaging based parameters and the *subacute deficit* for the prediction of the *residual deficit*. Again, the *subacute deficit* was the best predictor of the *residual deficit*, followed by the *segmented MRI* and the *lesion volume*. **E**, Analogous to the testing cohort, prediction of *residual deficit* was performed using an increasing number of regions in the *segmented MRI*. Dashed lines at $x=14$ and $y=21.5$ denote the local minimum of *PE* that had previously been observed in the testing cohort.